Turkish Journal of Earth Sciences (Turkish J. Earth Sci.), Vol. 21, 2012, pp. 315–334. Copyright ©TÜBİTAK
doi:10.3906/yer-1005-6 First published online 16 December 2010

Palaeoclimate Evolution in Siberia and the Russian Far East from the Oligocene to Pliocene – Evidence from Fruit and Seed Floras

SVETLANA POPOVA[1,2], TORSTEN UTESCHER[3], DMITRIY GROMYKO[1], ANGELA A. BRUCH[4] & VOLKER MOSBRUGGER[2,4]

[1] Komarov Botanical Institute / Laboratory of Palaeobotany, 2 Prof. Popova Street, 197376 Saint Petersburg, Russia (E-mail: celenkova@gmail.com)
[2] Biodiversity and Climate Research Centre (LOEWE BiK-F), Senckenberganlage 25, D-60325 Frankfurt, Germany
[3] Steinmann Institute, Bonn University, Nußallee 8, D-53115 Bonn, Germany
[4] Senckenberg Research Institute and Natural History Museum, Senckenberganlage 25, D-60325 Frankfurt, Germany

Received 11 May 2010; revised typescripts received 10 August 2010 & 15 November 2010; accepted 16 December 2011

Abstract: The Cenozoic continental deposits of Western Siberia, Eastern Siberia and the Russian Far East are best described on the basis of carpological records. The palaeoclimate evolution has been reconstructed quantitatively (Coexistence Approach) providing inferred data on temperature, precipitation and the mean annual range of these parameters. Climate curves document the transition from very warm and humid conditions in the Late Oligocene via the Middle Miocene Climatic Optimum to a cool temperate climate during the Pliocene. Compared with other time intervals the Miocene climate is the most comprehensively reconstructed. For the Middle Miocene the Siberian and Far Eastern data are combined with the 'NECLIME data set' available for the same time slice, thus allowing a synthesis and discussion of temperature and precipitation patterns on a Eurasia-wide scale. The MAT pattern on a Eurasia-wide scale shows a strong latitudinal temperature increase from the Russian Far East to China, and a well expressed longitudinal gradient from Western Siberia to warmer conditions in Europe, the Black Sea area and the Eastern Mediterranean. The reconstructed MAP of Western Siberia is around 1000 mm, which is close to the data obtained for the continental interior of Northern China but lower than most of the data in the Eurasian data set.

Key Words: Siberia, Russian Far East, Oligocene, Miocene, Pliocene, fruit and seed floras, palaeoclimate

Sibirya ve Rusya Uzak Doğu'sunda Oligosen'den Pliyosen'e Paleoiklim Evrimi – Meyve ve Tohum Floralarından Veriler

Özet: Batı, Doğu Sibirya ve Rusya Uzak Doğu'sunun Senozoyik karasal tortulları karpolojik (tohum-meyve) kayıtları temel alınarak en iyi şekilde tanımlanmıştır. Paleoiklim evrimi, sıcaklık, yağış ve bu parametrelerin yıllık ortalama uzanımlarından elde edilmiş verilere dayanarak sayısal olarak (Birarada Olma Yaklaşımı) yeniden düzenlenmiştir. İklim eğrileri, Geç Oligosen'den Orta Miyosen İklimsel Maksimum'a çok sıcak ve nemli koşullardan, Pliyosen süresince serin ılıman koşullara geçişi belgelemektedir. Diğer zaman aralıkları ile karşılaştırıldığında, Miyosen iklimi en kapsamlı olarak yeniden şekillendirilmiştir. Sibirya ve Uzak Doğu'su Orta Miyosen'i için veriler, Avrasya geniş ölçeğinde sıcaklık ve yağış modellemelerinin sentezi ve tartışmasını sağlayacak şekilde, benzer zaman dilimi için elde edilmiş 'NECLIME veri seti' ile biraraya getirilmiştir. Avrasya geniş ölçeğinde yıllık ortalama sıcaklık (YOS) modeli, Rusya Uzak Doğu'sundan Çin'e kuvvetli enlemsel sıcaklık artışı ve Batı Sibirya'dan Avrupa, Karadeniz alanı ve Doğu Akdeniz'deki daha ılık koşullara iyi ifade edilmiş boylamsal değişimi göstermektedir. Batı Sibirya'dan elde edilmiş yıllık yağış miktarı (YYM), Avrasya veri setindeki verilerin çoğundan daha düşük fakat Kuzey Çin'in kıta içinden elde edilmiş veriye yakın olup, 1000 mm civarındadır.

Anahtar Sözcükler: Sibirya, Rusya Uzak Doğusu, Oligosen, Miyosen, Pliyosen, meyve ve tohum floraları, paleoiklim

Introduction

The Western Siberian Basin is located between Novaya Zemlya and the Ural Mountains to the west, the Kazakh highlands to the south, and the East Siberian platform and the Taymyr fold belt to the east and the northeast, respectively. The basin covers over 3.5 million km^2 and represents a depocentre with important hydrocarbon resources, with a basin fill of several thousand metres of Mesozoic to Cenozoic strata resting on a folded Palaeozoic basement (Vyssotsky *et al.* 2006). The Cenozoic succession of Western Siberia comprises shallow marine platform sediments and, from the Oligocene on, predominantly fluviatile to lacustrine continental deposits (Arkhipov *et al.* 2005). While for the marine Palaeogene deposits dinocyst stratigraphy can be used for correlation (e.g., Kuz´mina & Volgova 2008), younger continental deposits are mainly dated by palaeobotanical means (e.g., Gnibidenko 2007). Thus, 17 floral complexes were established by Nikitin (2006), subdividing the time-span from the Rupelian to the earliest Pleistocene. From the Serravallian on, these flora complexes can partly be connected to mammal zones (Babushkin *et al.* 2001). The stratigraphic concept based on palaeocarpology is completed by palynological data (Babushkin *et al.* 2001) and magnetostratigraphic studies carried out in the Taganskaja (Kireevskoe locality) and the Besheulskaja Series, approximately corresponding to the Burdigalian to Serravalian time-span. As a result, a regional stratigraphical scheme was established allowing for correlations with the international standard (Babushkin *et al.* 2001).

The Russian Far East is located between Lake Baikal in Eastern Siberia and the Pacific Ocean. Our knowledge of the Cenozoic strata in Northeastern Siberia including the Far East is still limited. While in Western Siberia Cenozoic horizons can be traced over long distances, Cenozoic exposures in Northeastern Siberia and the Far East occur in isolated intramontane and marginal basins, hampering a correlation of the strata (Nikitin 2007). Stratigraphic subdivision and dating of the continental deposits in this area is mainly based on palaeobotanical means (Nikitin 2007).

At the beginning of the 20th century palaeobotanical research on the Cenozoic floras of Western Siberia began. Leaf floras primarily originate from Tomsk, Omsk, and Novosibirsk Oblasts and were studied by various researchers such as Kryshtofovich (1928), Chahlov (1948), Gorbunov (1955), and Yakubovskaya (1957). The most extensive studies were carried out by P. Nikitin, V. Nikitin (1999) and P. Dorofeev (1963) who worked on this subject throughout the 20th century. Owing to their common efforts the main composition of the Cenozoic floras of Western Siberia and northeastern Russia (including the Far East) was revealed and evolution stages of the flora were defined. According to this there are four main evolution stages in the Cenozoic floras of Siberia (Nikitin 2006). In the first phase, the pre-Turgayan, a subtropical flora existed (Late Cretaceous–Eocene). The second, Turgayan, phase is characterized by the expansion of a boreal, warm temperate flora. This flora evolved during the Early Oligocene and, during the Late Oligocene to Early Miocene, was replaced by diverse mesophilous mixed coniferous-broad-leaved forests. The next phase, Post-Turgayan (Middle and Late Miocene to Early Pliocene), mainly shows the dominance of forest-steppe and steppe landscape later on. The last phase is the modern stage which started at the end of the Pliocene.

Palaeocarpological studies of the Cenozoic deposits in Northeastern Siberia and the Far East began in the 1960s. They were complicated by uncertainties in the stratigraphical position of the flora bearing horizons, by the mostly poor preservation of the fruits and seeds (Nikitin 2007). Also, sediments are often diagenetically altered making preparation of the fossils difficult (Nikitin 1969). As a consequence the knowledge about composition and evolutionary history of the Cenozoic flora of Northeastern and the Far East is limited (Nikitin 2007). Filling gaps on the map of Siberia and northeastern Russia by discovering new localities and identifying fossil taxa were one of the main objectives of Russian palaeobotanical research during the middle of the 20th century.

The Cenozoic palaeoclimate evolution of Europe is relatively well investigated. Recent studies unravel continental climate change during the Neogene of China. However, only little information is available for the high latitudes of northern Eurasia.

The climate evolution of the Neogene of Western Siberia has been outlined by Nikitin (1988) but was based only on qualitative interpretations of the floral record. A qualitative palaeoclimate record for the Cenozoic of the Arctic coastal areas of northeastern Siberia (Kolyma River Basin) based on pollen flora was published by Laukhin *et al.* (1992). The Nikitin (1988) climate curve displays a long-term cooling trend from warmest conditions at the Oligocene/Miocene transition to a colder climate in the Late Pliocene. During the Miocene this cooling is connected to drying while for the Pliocene several fluctuations from humid to dry are displayed. However, the data given by Nikitin (1988) are not informative enough to draw conclusions about climate types existing in the single stages.

Lunt *et al.* (2008) suggested that the high latitudes are a target region, where proxy data should be acquired. It is relevant because anything that happens with climate seems to affect the higher latitudes. Here we present a first quantitative reconstruction of the Cenozoic palaeoclimate evolution for this region.

Materials and Methods

In the present study a total of 91 Cenozoic fruit and seed floras from western and northeastern Siberia and the Russian Far East are selected from published sources and analysed with respect to palaeoclimate (Table 1). The individual floras comprise 14 to 198 taxa. For each of the fruit and seed floras studied, the floral diversity, geographical position and stratigraphical dating are given in Appendix 1. These data were published by Nikitin (2006) in his monograph on the seed and fruit flora of Siberia. Three Middle Miocene floras from the Tambov oblast, in European Russia, are also included in the analysis. Flora lists for these sites were published by Dorofeev (1963).

The Cenozoic deposits of northeastern Siberia have been little investigated. The biostratigraphy of the Cenozoic continental deposits of Western Siberia is better known. So far, mainly palaeobotanical data have been used to subdivide the succession. A system of flora complexes serves as a basis for the regional stratigraphical chart recently developed (Figure 1). This stratigraphical scheme can be correlated with the palynological and palaeomagnetic zonation of Siberia (Gnibidenko *et al.* 1989; Nikitin 1999; Martynov *et al.* 2000).

Table 1. Mean taxa diversity of singles floras for each time interval from Late Pliocene to Early Oligocene.

Time slice	Number of floras	Mean taxa diversity
Late Pliocene	10	56
Early Pliocene	2	22
Late Miocene	7	36
Middle Miocene	15	58
Early Miocene	32	56
Late Oligocene	19	83
Early Oligocene	24	45

To study the palaeoclimate evolution from the Early Oligocene to the Late Pliocene in different parts of Siberia, the Russian Far East and Tambov oblast (European Russia) the Coexistence Approach (CA) was used (Mosbrugger & Utescher 1997). The CA follows the nearest living relative concept. It is based on climatic requirements of modern plant taxa that are identified as Nearest Living Relatives (NLRs) of the fossil taxa recorded. Climate data for extant plants are obtained by overlapping plant distribution area and modern climatology. Fossil plant taxa and climatic requirements of their NLRs are made available in the Palaeoflora (www.palaeoflora.de) data base (Utescher & Mosbrugger 2010). Coexistence intervals for different climatic parameters can be calculated using the program Climstat. They define ranges of climate variables that allowed most considered plant taxa to co-exist at the location studied.

To apply the CA to the Siberian, Russian Far East and Tambov floras, major extensions of the Palaeoflora data base are necessary. A total of about 270 fossil taxa had to be entered including information on organ type, stratigraphic range, reference, and NLRs cited. Climate data for about 160 modern taxa, both species and genera, not so far available in the Palaeoflora had to be retrieved. This was done by overlapping plant distribution areas and climatology (Müller 1996).

The NLR concept provided by Nikitin (2006) was checked. For fossil taxa occurring earlier than the Late Miocene, NLRs were preferably identified at the generic level; for younger records a comparison with a single modern species partly makes sense, e.g., for *Acorus calamus L.*, *Alnus cordata* (Loisel.) Loisel., *Aralia spinosa* Vent., *Comptonia peregrina* L., *Hippuris vulgaris* L., *Sambucus racemosa* L., *Styrax japonica* Zieb. et Zucc.. For *Sciadopitys* and *Sequoia,* known to be problematic in the applications of the

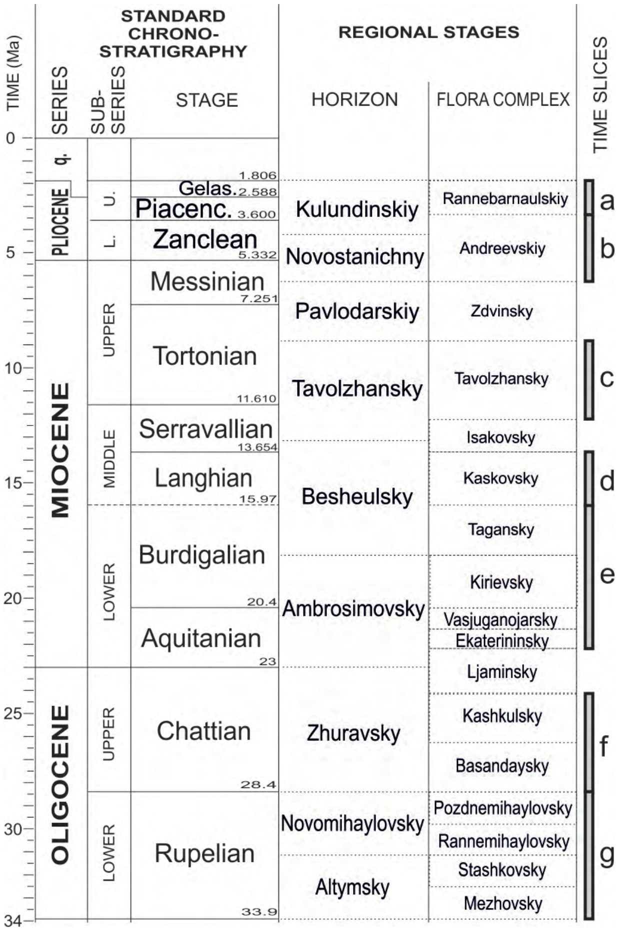

Figure 1. Standard chronostratigraphy based on Gradstein *et al.* (2004) and the International Stratigraphic Chart, 2006 (ICS). The correlations with Western Siberian regional stages (horizons) and fauna complexes follow Babushkin *et al.* (2001) and Nikitin (2006). Time intervals defined for the present study: a– Late Pliocene, b– Early Pliocene, c– Late Miocene, d– Middle Miocene, e– Early Miocene, f– Late Oligocene, g– Early Oligocene.

CA on Cenozoic floras (cf. Utescher *et al.* 2000), climate data for the plant family are used. Both taxa are relics and had a much wider distribution in the Cenozoic than at present. The genera *Scindapsus* and *Urospatha* were excluded from the analysis, because these present-day tropical elements were common in the mid-latitude Cenozoic carpological record and generally formed climatic outliers in the CA analysis (e.g., Utescher *et al*. 2000).

Floras were analysed with respect to 3 temperature and 3 precipitation variables: mean annual temperature (MAT), mean temperatures of the coldest and warmest months (CMT; WMT), mean annual precipitation (MAP), and mean precipitation of the wettest and the driest month (MPwet; MPdry). These 6 climate variables were calculated independently for all floras studied, and then the resulting set of 6 CA ranges was used to calibrate data using modern climate space. Thus refined, narrower intervals could be obtained, leading to a more precise reconstruction. Details of the procedure are described in Utescher *et al.* (2009).

To illustrate climate change in Siberia, the Russian Far East and Tambov oblast during the Cenozoic, the floras are allocated to 7 time intervals (cf. Figures 1–4). Time intervals are defined according to the international standard: Early and Late Oligocene, Early, Middle, and Late Miocene, and Early and Late Pliocene. This allocation of the floras was performed using the system of flora complexes (Nikitin 2006). In Western Siberia Figure 1 shows how these flora complexes approximately correlate with the chronological standard (Babushkin *et al.* 2001; cf. chapter 1). As is obvious from the figure, there is some overlap of complex and stage boundaries, e.g., for the Late Miocene (later Serravallian to late Tortonian) and the Late Pliocene time interval (Piacenzian to earliest Pleistocene), stratigraphic uncertainties that cannot be overcome when considering the available stratigraphic concept, but that are still acceptable, we think, in view of the coarse resolution chosen for the time intervals studied. More details about the stratigraphic positioning of the sites are available in Appendix 1 where flora complexes are cited for each flora, where known.

To visualize the results, a series of maps is provided and discussed below showing the evolution of the 6 climate variables analysed in 7 stages throughout the Cenozoic. For the technical preparation of the maps ArcView 3.2 was used. The grid was generated using the following settings of Spatial Analyst: method IDW; power 2.

Results

Palaeoclimate data, presently reconstructed for 6 different climate variables (mean annual temperature, cold, warm month mean, mean annual precipitation, annual range of temperature and precipitation) are

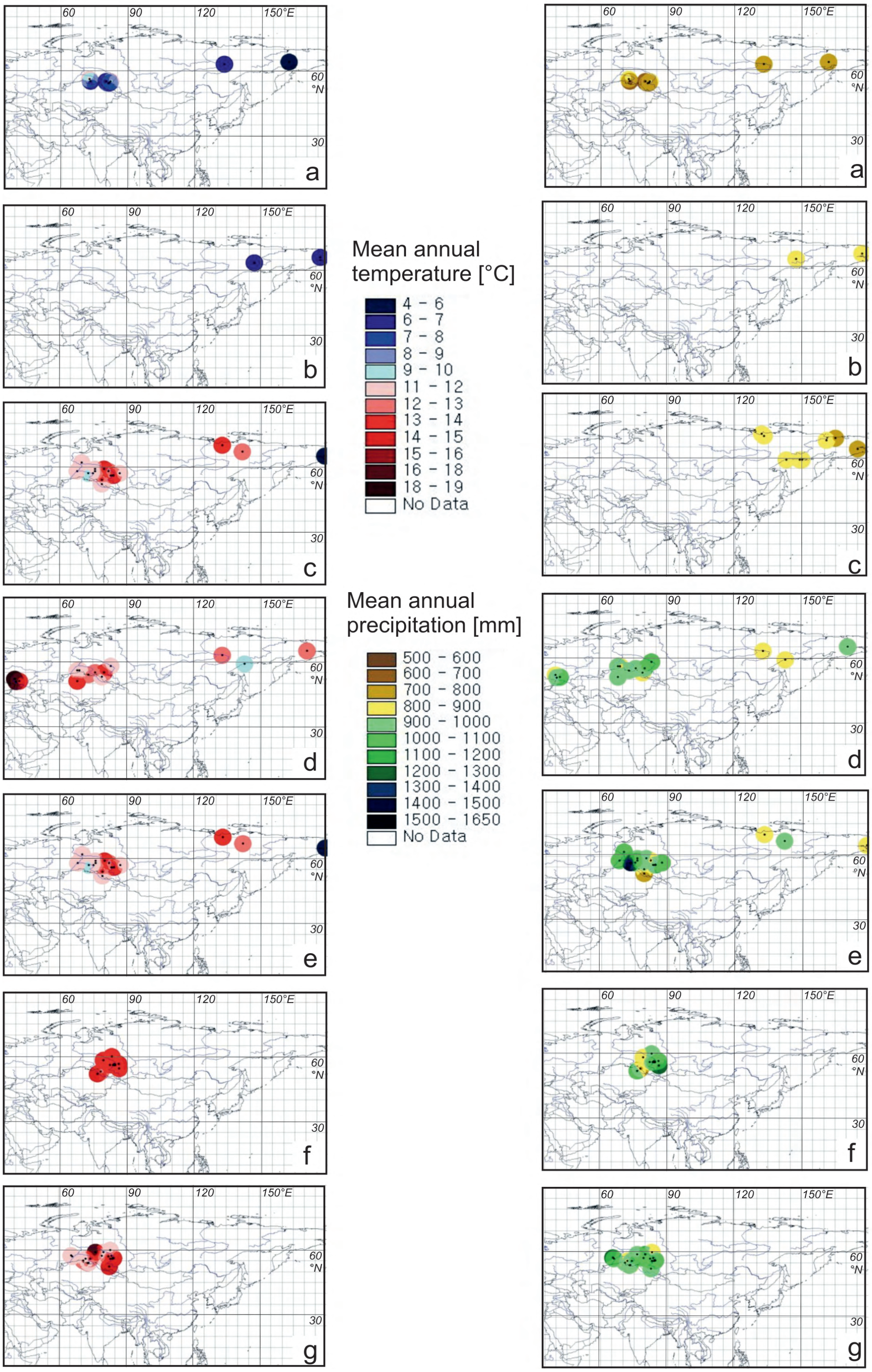

Figure 2. Mean annual temperature (left) and mean annual precipitation (right) in the Cenozoic of Western, Eastern Siberia and the Russian Far East: a– Late Pliocene, b– Early Pliocene, c– Late Miocene, d– Middle Miocene, e– Early Miocene, f– Late Oligocene, g– Early Oligocene.

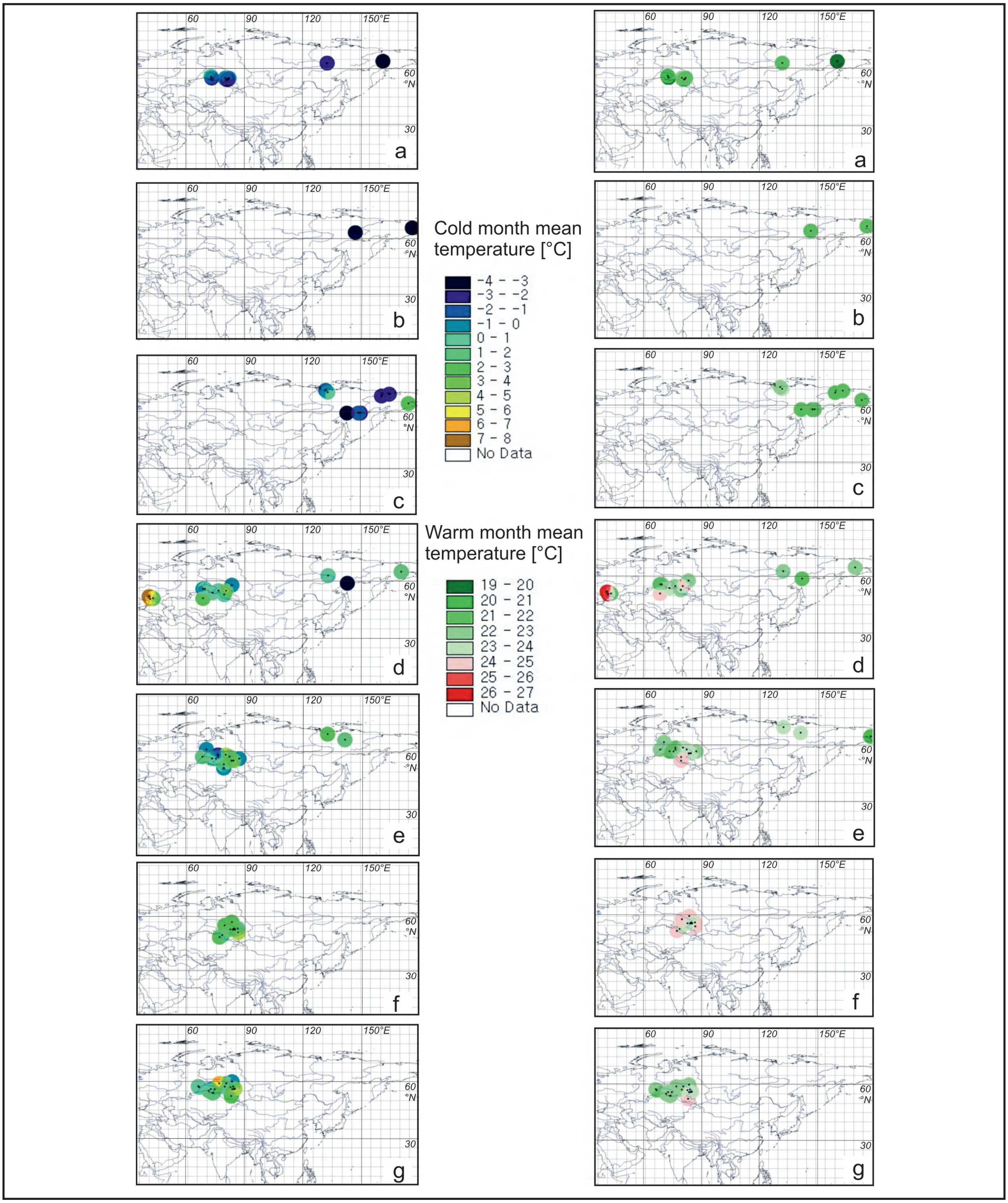

Figure 3. Cold month mean temperature (left) and warm month mean temperature (right) in the Cenozoic of Western, Eastern Siberia and the Russian Far East: a– Late Pliocene, b– Early Pliocene, c– Late Miocene, d– Middle Miocene, e– Early Miocene, f– Late Oligocene, g– Early Oligocene.

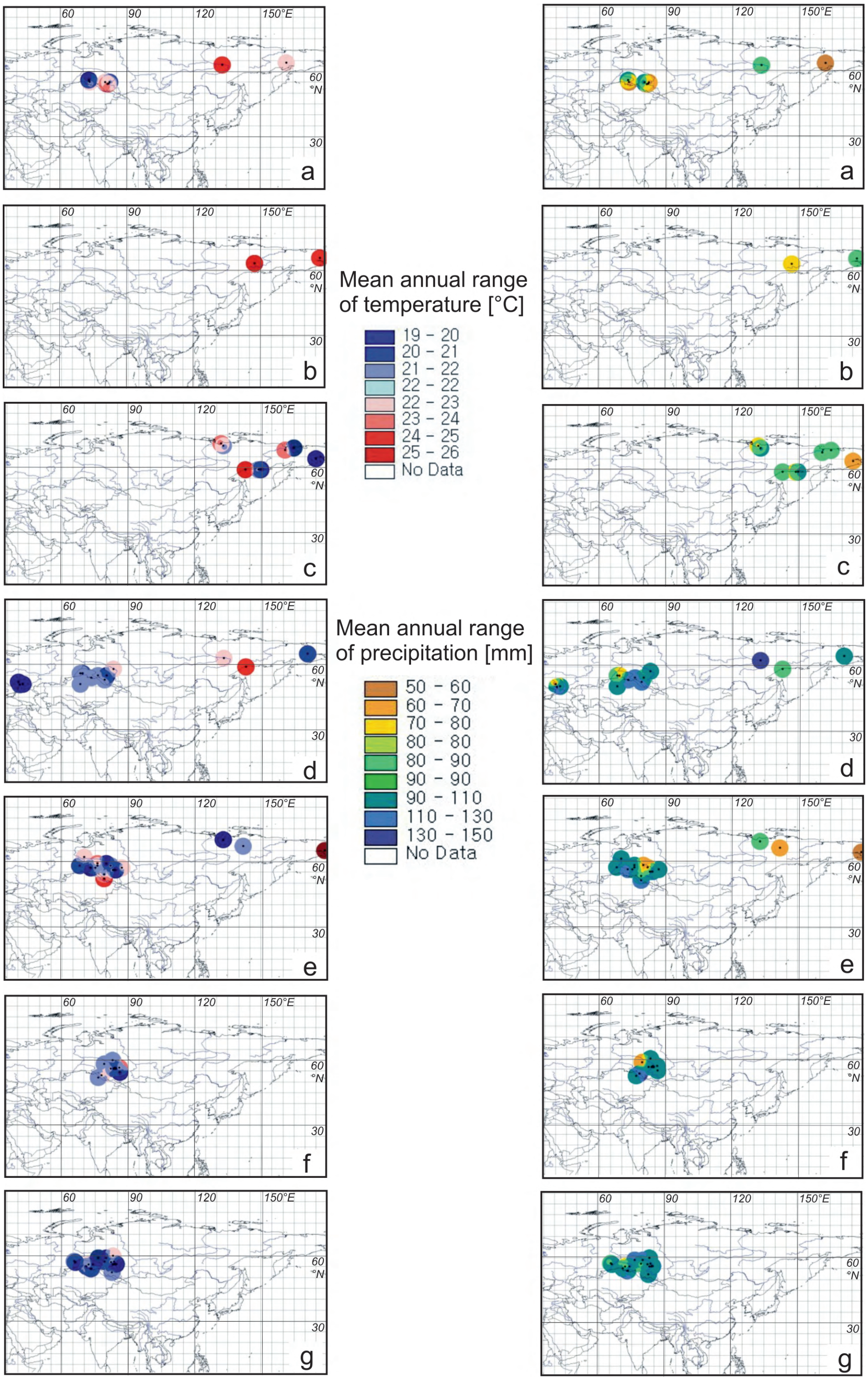

Figure 4. Mean annual range of temperature (left) and mean annual range of precipitation (right) in the Cenozoic of Western, Eastern Siberia and the Russian Far East: a– Late Pliocene, b– Early Pliocene, c– Late Miocene, d– Middle Miocene, e– Early Miocene, f– Late Oligocene, g– Early Oligocene.

shown in the map series for 7 time intervals. The maps allow an analysis of climate change in Siberia, the Russian Far East and Tambov oblast during the Cenozoic in time and space. Gradients and patterns obtained for single climate variables are shown in Figures 2–4 and described below. Means of climate variables in each time interval obtained for Western Siberia and the Russian Far East are given in Table 2.

For Western Siberia changing climate patterns can continuously be studied for the time-span from the Early Oligocene to the Middle Miocene. In the latter time interval data for Kazakhstan are also available. While for the Late Pliocene several data points are present, the Late Miocene and Early Pliocene situation cannot be documented. For Eastern Siberia and the Far East climate evolution is documented for the time-span from the Early Miocene to the Late Pliocene.

Temperature

In the temperature evolution of Western Siberia during the Oligocene, the highest values are indicated by the Early Oligocene Trubachovo and Katyl'ga floras (Appendix 1), with MAT up to almost 17.3°C, CMM at 6.6°C, and mean WMM at 24.7°C. The Early Oligocene Kompasskiy Bor flora (Appendix 1), Western Siberia, in contrast, has the lowest temperature results with 10.5°C for MAT, 0.05°C for CMM, and 23.3°C for WMM when Ca interval means are regarded. When averaged across all Early Oligocene floras a MAT of 13.5°C was indicated, while the mean for the Late Oligocene is about 14°C, thus indicating a temperature increase (Table 2). When comparing the means from MAT, CMT, and WMT, slightly cooler conditions during the Oligocene/Miocene transition are indicated for Western Siberia floras.

In the Early Miocene this cooling trend continued. Comparatively low temperature means are indicated for the Koinatkhun flora (Appendix 1) in the Far East, due to the low diversity of the flora with only 9 taxa contributing to the climate data in the analysis (with 8 taxa being the limit in the CA). CA intervals obtained are quite large, thus allowing also for warmer conditions (MAT: –6.2–16.1°C; CMT: –26.8–6.4°C; WMT: 15.9–25.6°C). The mean values of MAT reconstructed for the Western Siberian floras (12.9°C) are about 2°C lower than the data from the Far East (10.45°C). A more pronounced contrast between both regions is evident from CMT, with a mean of –5.05°C obtained for the Far East and 2.5°C for Western Siberia.

The slightly cooler Early Miocene conditions were followed by a minor temperature rise during the Middle Miocene. In the western part of Western Siberia MAT was around 13.6°C, but the Far East flora yield a MAT of 12.05°C. For example, MAT calculated for the West Siberian Orlovka flora (Appendix 1) ranges from 13.3 to 17.5°C and CMT from –0.1 to 7.7°C. For the Mamontova Gora and Rezidentsiya floras of Eastern Siberia (Appendix 1) MAT ranges from 12.7 to 13.7°C and 3.4 to 16.1°C, respectively (CMT: –0.1–1.3°C / –12.9–6.4°C). Data obtained

Table 2. Regional climate means by time interval.

Stage	Number of floras	MAT		CMM		WMM		MAP		Mpwet		MPdry	
		mean W Siberia	mean Far East	mean W Siberia	mean Far East	mean W Siberia	mean Far East	mean W Siberia	mean Far East	mean W Siberia	mean Far East	mean W Siberia	mean Far East
Late Pliocene	10	8.32	6.3	-2.01	3.3	18.2	20.6	751.46	749.5	105.75	107	28.8	29.25
Early Pliocene	2		7.22		-3.35		22.05		859		113.25		30
Late Miocene	7		9.66		-1.51		21.74		864.71		117.42		115.7
Mid-Miocene	15	13.6	12.05	2.86	2.57	24.1	22.6	965	867	149.4	140.5	44.8	37
Early Miocene	32	12.9	10.45	2.5	5.25	23.9	22.7	994.06	896.83	143.15	117.16	39.86	45.8
Late Oligocene	19	14.13		2.88		24.48		1015.6		145.36		42.97	
Early Oligocene	24	13.52		3.13		23.71		1029		139.79		37.5	

for the Middle Miocene floras of the Tambov oblast (European Russia) indicate the warmest conditions observed in our data. For example, one of the floral MAT ranges from 15.7 to 20.8°C, CMT from 2.2 to 13.6°C, and WMT from 25.6 to 28.1°C.

The onset of pronounced cooling is quite evident in the Late Miocene temperature data obtained from Eastern Siberia, with MAT at 10.8°C, and from the Far East, with mean MAT at 9.36°C. The Late Miocene Eastern Siberia Omoloy river flora (Appendix 1) is characterized by a MAT range from 7.3 to 16.1°C, with a CMT of –3.8°C, while for the Temmirdekh-khaya flora (Appendix 1) nearby, MAT ranges from 9.3 to 10.8°C, CMT from –2.8 to 1.1°C and WMT from 21.6 to 23.8°C. Results obtained from the other Late Miocene floras of the Far East show MAT ranging from 2.42 to 16°C, CMT from –9.7 to 7°C and WMT ranging from 17.6 to 25.6°C, indicate a cooling trend.

The Early Pliocene MAT reconstructed for 2 data points in Eastern Siberia and the Russian Far East were lower by more than 2°C than in the Late Miocene, testifying to continuing cooling. Late Pliocene floras of the Far East are characterized by MAT around 6°C and thus indicate only a slight declining trend when compared to Early Pliocene conditions, characterized by MAT around 7°C as calculated for the Eastern Siberia Delyankir flora (appendix 1) with a MAT result 6.9–7.8°C. However, for CMM a marked temperature decrease from the Early to the Late Pliocene is evident from the data. In Western Siberia MAT had clearly dropped below 10°C in the Late Pliocene; for most of the floras MAT means from 6°C to 8°C result, except for the flora of Merkutlinskiy where a MAT around 11°C was obtained. Winter temperatures reconstructed for all Pliocene localities were well below freezing point, contrasting the Middle Miocene conditions.

Precipitation

To study precipitation patterns in Western and Eastern Siberia and the Russian Far East, mean annual precipitation (MAP) and the mean annual range of precipitation (MARP– calculated as difference of MPwet and MPdry) were calculated by the CA for the time intervals studied. The MAP of Early and Late Oligocene floras of Western Siberia (Table 2) stayed about at the same level, with values ranging from 1015 to 1029 mm. For the Rupelian Kompasskiy Bor flora (Appendix 1), a MAP interval from 776 mm to 864 mm was obtained; for Obukhovka and Pavlograd (Appendix 1) 592 mm to 1146 mm and 820 mm to 869 mm were obtained respectively, with the latter values being the lowest registered in our Oligocene record. Precipitation rates of the wettest month (MPwet) calculated for the Rupelian Achair flora (Appendix 1) range from 150 mm to 195 mm. The driest month precipitation (MPdry) of the late Rupelian Antropovo flora (Appendix 1) ranges from 53 mm to 64 mm. During the Late Oligocene there is a slight increase of observed precipitation rates. For the Dubovka flora (Appendix 1) MAP ranges between 1146 and 1322 mm, MPwet from 150 to 170 mm, and MPdry from 41 to 64 mm.

The mean MAP determined for the Early Miocene floras of Western Siberia is 994 mm. The wettest Western Siberia site is Gorelaya (Appendix 1) with MAP ranging from 760 to 3151 mm, MPwet around 389 mm and MPdry from 90 to 165 mm. For Early Miocene floras in the Far East a MAP of around 896 mm was obtained. Slightly drier conditions are indicated by the Ulan-Kyuyugyulyur flora of Eastern Siberia (MAP 592–1206 mm; MPwet 143 mm) and the Far Eastern Koynatkhun flora (MAP 406 – 1206 mm; MPwet 64–143 mm). In the Middle Miocene, precipitation rates tend to show no significant change when compared to the Early Miocene level, as for the Tambov oblast and the Western Siberian floras. However, for the Mamontova Gora flora in Eastern Siberia a slight decreasing trend is shown, with MAP ranging from 776 to 847 mm and MPdry being around 32 mm.

Results from the Late Miocene to Early Pliocene floras of the northeastern part of Eurasia show a continuing trend to drier conditions. For instance, MAP reconstructed for the Late Miocene Osinovaya flora, in the Far East, ranges from 609 to 975 mm, for the Tnekveem flora (Appendix 1) a MAP of at least 373 mm is indicated. Lowest MPDry rates with a CA range from 9 mm to 26 mm are obtained for Late Miocene Magadan flora. Annual precipitation rates reconstructed for the Late Pliocene floras of West Siberia are 751 mm at a mean, for Far Eastern floras comparable values are calculated (749 mm at a mean). The northern Late Pliocene flora of Blizkiy, Far East, (Appendix 1) shows the driest conditions, with MAP ranging from 453 to 980 mm, MPwet from 68 to 118 mm, and MPdry from 8 to 53 mm.

Discussion

Cenozoic Palaeoclimate Evolution of Siberia

The evolution of temperature patterns of Western and Eastern Siberia and the Russian Far East during the second half of the Cenozoic largely coincides with the major trends of global climate evolution, as reflected in the marine oxygen isotope record (e.g., Zachos *et al.* 2001) and in continental climate curves (e.g., Paratethys: Utescher *et al.* 2007; NW Germany: Utescher *et al.* 2009). Mean values calculated for Western and Eastern Siberia and the Russian Far East (Table 2) show that temperatures increased from the Early to the Late Oligocene (Western Siberia) followed by a slight decrease in the Early Miocene (Western Siberia). The slightly higher values obtained for the Late Oligocene might be related to the Late Oligocene warming at around 25 Ma known from marine records (Zachos *et al.* 2001). As well as in Western Siberia, a slight temperature decrease in the Early Miocene is not only documented in marine records but also in continental curves of Western Europe (e.g., Lower Rhine Basin; Utescher *et al.* 2009).

Mean temperature data reconstructed for both Western and Eastern Siberia indicate warmer conditions for floras allocated to the earlier part of the Middle Miocene (cf. Kaskovsky flora complex, Table 2). Thus the Middle Miocene Climatic Optimum (MMCO) known both from global marine records and from European continental curves (e.g., Zachos *et al.* 2001; Mosbrugger *et al.* 2005) is most probably reflected by the Siberian data. For Eastern Siberia and the Far East the onset of the subsequent Late Miocene Cooling and continuing temperature decrease during the Pliocene is clearly shown by our data (Table 2; Far East data column). In Europe, the Late Miocene Cooling is connected to an increase in seasonality of temperature (Utescher *et al.* 2000, 2007; Bruch *et al.* 2011). This is also evident from the data obtained from Eastern Siberia and the Far East (Figure 2a–e).

Comparison with Neighbouring Areas

Data cover allows a comparison of the Siberian data set with spatial palaeoclimate data reconstructed for adjacent continental areas of Eurasia in the three Miocene time intervals considered here. When our Early Miocene climate data reconstructed for Western Siberia is compared with available palaeoclimate data from Kazakhstan and Northern China, a steep gradient to warmer / wetter conditions towards the South and Southeast is evident (Table 2; Bruch & Zhilin 2006; Liu *et al.* 2011). MAT means calculated from the floras of the Far East and Western Siberia range from about 10°C to 13°C while Kazakhstan floras are warmer by 5–6°C; floras from Northern China are warmer by even 7–9°C. CMT and WMT reconstructed for Western Siberian floras show that conditions were cooler by about 3°C in Kazakhstan and by about 5°C when compared to Northern China. Drier conditions existed in Western and Eastern Siberia and in the Russian Far East, with mean MAP at 994 mm and 896 mm, respectively, whereas wetter conditions were observed for Kazakhstan (1077 mm) and from the floras in Northern and Western China, ranging from 1173 mm to 1111 mm).

In the Middle Miocene, the Siberian data are combined with the 'NECLIME data set' available for the same time interval (Bruch *et al.* 2007; Bruch *et al.* 2011; Liu *et al.* 2001; Utescher *et al.* 2011; Yao *et al.* 2011). The Eurasia-wide MAT pattern shows a strong latitudinal temperature increase from Far East Russia to China, and a well expressed longitudinal gradient from Western Siberia to warmer conditions in the West, the Black Sea area and the Eastern Mediterranean (Figure 5). Mean annual precipitation of Western Siberia, around 1,000 mm, is lower than other data reconstructed for most Middle Miocene Eurasian sites. Only floras located in the continental interior of Northern China provide values at a comparable level (Figure 6).

With smaller-scale regional patterns and trends of climate evolution both Far Eastern and Siberian floras, as well as the floral record of Northern China (Liu *et al.* 2011) show evidence of a slight temperature increase from Early to Middle Miocene. In Northern China this warming was connected to precipitation increase while in our study area MAP stayed at the same level. Results obtained from Middle Miocene floras of the Ukrainian Carpathians and Ukrainian

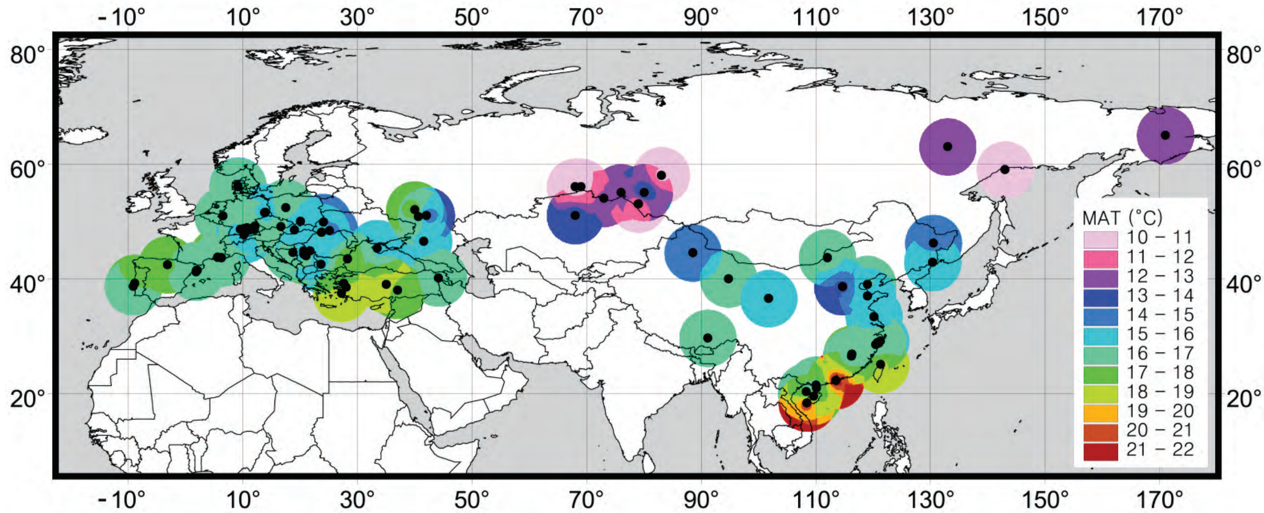

Figure 5. Mean annual temperature reconstructed for the combined Eurasian data set of the NECLIME network for the Middle Miocene time slice.

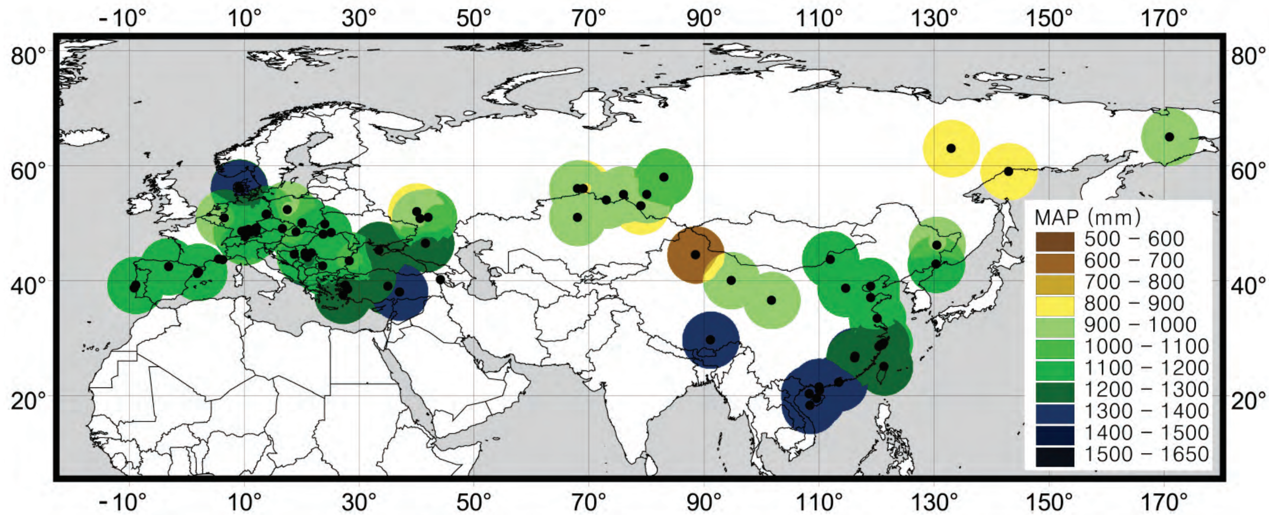

Figure 6. Mean annual precipitation reconstructed for the combined Eurasian data set of the NECLIME network for the Middle Miocene time slice.

Plain (Syabryaj *et al.* 2007) are also interesting to compare with floras of the European part of Russia in our data set (Tambov oblast). The mean values of MAT from the Ukrainian Carpathians and the Tambov oblast indicate similar temperature conditions at about 16–17°C, while values from the Ukraine Plain are lower by more than 4°C. The same observation can be made for CMT. This decreasing trend is most probably connected to a significant northward shift of the tectonic plate (Syabryaj *et al.* 2007). Drier conditions, with mean 974 mm are indicated by the floras of the Tambov region, when compared to those of the Ukrainian Carpathians (1179 mm) and Ukraine Plain (1202 mm). This result coincides very well with palaeoclimate studies based on large mammal hypsodonty, which indicate that more arid conditions became established in the mid-latitudes of the continental interior of Eurasia in the later Middle Miocene (Eronen *et al.* 2010).

As observed for the Middle Miocene (see above), Late Miocene data reveal the same latitudinal gradient from drier conditions in the Far East, with mean MAP at 864 mm to 1058 mm calculated for floras of Northern China (Liu *et al.* 2011). A comparable latitudinal gradient is obvious for MAT, which is over 5°C higher in Northern China.

Comparison with Present-day Climate Patterns

Present-day climate patterns over Siberia show a strong imprint of the Siberian High (SH), the strongest semi-permanent high pressure system of the Northern Hemisphere. The high plays a critical role in the climate over Eurasia and the Northwest Pacific through the formation of a cold and dry continental air mass in the cold season (Takaya & Nakamura 2005). Northern Siberia has the lowest winter temperatures on the globe, an extremely high seasonality of temperature and comparatively low MAP, with the highest precipitation rates during the summer. Present-day climatology (e.g., New *et al.* 2002) shows that the coldest conditions for MAT (<−20°C) and CMT −40°C) are recorded in Eastern Siberia. This is also true for MART doming up in the coastal areas near the Laptev Sea. Climate data show a steep latitudinal gradient to warmer conditions in the south and shallower longitudinal gradients towards the west and somewhat more pronounced ones towards the Far East (cf. present-day climatology, New *et al.* 2002).

An imprint of the SH is also evident in MAP gradients over Eastern Siberia (cf. present-day climatology, New *et al.* 2002). MAP is lowest in the centre of the anticyclone (<300 mm). It shows a steep latitudinal gradient towards wetter conditions from the Arctic coastal areas to the coastal area of East Asia. Towards the West, MAP steadily increases, reaching 500 to 600 mm in Western Siberia and 600 to 700 mm in Eastern Europe. This simple pattern is, however, complicated by a gradient to dry conditions in the continental interior of Eurasia comprising most of Kazakhstan, Mongolia and Western China. South of ca. 50 to 55°N latitude, MAP rapidly declines below 400 mm. In the seasonal distribution of rainfall, the climate over Siberia is dry in winter, with the wettest month commonly being August. During summer the Pacific coastal areas of the Far East are influenced by the East Asian monsoon.

The SH predominantly originates from radiative cooling of the continental area during winter, and its intensity thus correlates closely with local surface air temperature (Panagiotopoulos *et al.* 2005) The strength of the SH has a strong impact on the large-scale atmospheric circulation patterns over Eurasia. In Eastern Eurasia, it is known that both Arctic oscillation (AO) and the intensity of the SH strongly affect the East Asian winter monsoon and the outbreak of cold air masses into East Asia (e.g., Gong *et al.* 2001). However, the SH strongly influences winter temperatures over the mid-latitudes of Western Eurasia because the high can extend westwards and thus block lows coming in from the west (Rogers 1997).

Due to the data cover the climate patterns obtained for the past time intervals are fragmentary. However, it is clearly evident that warm and wet climate conditions prevailed in the study area between the Early Oligocene and the Mid-Miocene, with CMTs commonly above 0°C. The Middle Miocene temperature gradients have the same sense as today but are shallower by ca. 80 % (Figure 2, Table 2). MART increases from Kazakhstan (mean ca. 19°C) towards Western Siberia (mean ca. 22°C) and Eastern Siberia (Mamontova Gora flora: 23°C), decreasing again towards the Far East (Osinovaja flora: 22.5°C). CMT shows a parallel pattern. This clearly indicates that up to the Middle Miocene, atmospheric circulation patterns substantially differed from present-day conditions and no strong anticyclone existed over Siberia during the cold season.

During the Late Miocene no data are available for Western Siberia, but the results obtained from Eastern Siberia and the Far East for the first time show a higher CMT difference of ca. 7°C between the Far Eastern Osinovaja site (3°C) and the Omoloy High Arctic site −4°C), attaining ca. 30% of present-days gradient (−20°C / −47°C). At the same time winter temperatures clearly below freezing point are indicated. Western Siberia experienced significant drying during the Late Miocene Cooling (cf. Middle

Miocene and Late Pliocene MAP data on Figure 2a, d). Thus it is probable that during the Late Miocene, with an intensifying Arctic glaciation (e.g., Thiede *et al.* 1998), circulation patterns in the NH started to shift to present-day conditions, although temperatures were still considerably higher than today and gradients much weaker. This observation is in agreement with proxies from other high latitude regions such as palaeobotany-based data obtained for the Late Miocene Homerian group of Alaska revealing a warmer climatic aspect than previously thought (Reinink-Smith & Leopold 2005).

Thus the above findings largely coincide with the observation that the intensification of the East Asian winter monsoon did not occur prior to the Late Miocene (at ca. 8 Ma; cf. Qiang *et al.* 2001; Fan *et al.* 2006). The establishment of this pattern was accompanied by the onset of drying in the mid-latitude continental interior of Eurasia and the expansion of C4 plants in the Himalayan foreland from the later Late Miocene on (Fortelius *et al.* 2002; Guo *et al.* 2004; Huang *et al.* 2007). This evolution is also linked to the uplift history of the Tibetan Plateau, reinforcing the climatic gradients over Eastern Eurasia. Tibetan uplift has strong pulses between the Late Miocene and the Late Pliocene, as shown by coarse-gained continental sediments and sedimentary records from ODP sites in the Pacific (Zhang *et al.* 2007).

Our data show that drying and cooling intensified in the study area during the Pliocene. However, the available data cover of both time intervals does not permit a detailed view. In Northeast China, possibly more temperate and more humid conditions persisted at the same time (Badaogou flora, Jilin; cf. Stachura-Suchoples & Jahn 2009; Kovar-Eder & Sun, 2009). According to recent dating a Pliocene age of this diverse, warmth-loving flora cannot be excluded (Sun Ge, personal communication 2010).

So far General Circulation models have difficulties in simulating palaeo-conditions with very warm and partly ice-free high northern latitudes (e.g., Knies & Gaina 2008) under an only moderately raised atmospheric CO_2 level (Micheels *et al.* 2007, 2009; Steppuhn *et al.* 2007). Nevertheless, model studies provide clues for possible triggering mechanisms. A warming mechanism, e.g., the presence of polar stratospheric clouds, was proposed by Sloan and Pollard (1998) causing up to 20°C warming of high latitude winter temperatures in the model. Modelling studies for a Tortonian time interval point to enhanced subtropical jets and increased storm track activity between 40°N and 60°N, as well as higher fluxes in the sensible and latent heat, leading to a significant warming of the high latitudes. It is shown that a complete forest cover of the high latitudes that replaces modern tundra vegetation in the model affects albedo and the hydrological cycle, thus leading to warmer and wetter conditions in the polar region (Micheels *et al.* 2007, 2011).

Summary and Conclusions

Our results show that the warmest and wettest conditions in Western Siberia existed during the Oligocene, with MAT around 14°C, and MAP at 1000 mm, while Early Miocene data indicate slight cooling and drier conditions. In the Middle Miocene temperatures increased again while the decreasing trend of precipitation continued. In Eastern Siberia and the Russian Far East subsequent cooling began in the Late Miocene. For the Late Pliocene mean MAT around 6°C is indicated. MAP shows a significant decreasing trend from the Early Miocene on. The most marked drying (by over 100 mm) occurred in the Late Pliocene.

Our data significantly contribute to recent, quantitative palaeoclimate reconstruction for the Cenozoic of Eurasia based on the palaeobotanical record. These quantitative climate data for continental areas are essential for the validation of the results obtained from palaeoclimate modelling. When combined with NECLIME data sets, comprising localities all over Eurasia, climate patterns and their changes throughout the Cenozoic can be studied, for the first time also including the higher latitudes of Eastern Eurasia. In the present study this is done for the Middle Miocene: Eurasia-wide reconstruction for other Cenozoic time slices will follow.

Currently work is in progress to reconstruct the vegetation evolution of Siberia and the Russian Far East, using the same localities and time intervals. Thus, it will be possible to reconstruct the full pattern of biodiversity evolution for the Siberian territory related to climate change in the time-span from the Oligocene to the Pliocene.

Acknowledgments

We thank our colleagues A. Micheels and E. Herzog for many fruitful discussions. Special thanks are due to V.P. Nikitin for help in understanding questions of Western Siberian stratigraphy. We are indebted to M. Fortelius, Sun Ge, and C. Liu for carefully reviewing our manuscript, and for their kind advice on how to improve it. This work would not have been possible without the financial support granted by DAAD (A/08/80543) and we also thank the federal state of Hessen (Germany) within the LOEWE initiative (Bik-f (E. 1.12 R80573)) for the chance to continue this study. This work is a contribution to the program 'Neogene Climate Evolution in Eurasia – NECLIME'.

References

Arkhipov, S.A., Volkova, V.S., Zolnikov, L.D., Zykina, V.S., Krukover A.A. & Kul´kova, L.A. 2005. West Siberia. *In*: Wright, Jr. H.E., Blyakharchuk, T.A., Velichko, A.A. & Borisova, O. (eds), *Cenozoic Climatic and Environmental Changes in Russia*. Geological Society of America Special Paper **382**.

Babushkin, A.E., Volkova, V.S. & Gnibidenko, Z.N. 2001 (eds). *Unified Regional Stratigraphic Charts of Neogene and Paleogene Deposits of the West Siberian Plain and Explanatory Note* [in Russian], Novosibirsk, **82**.

Bruch, A. & Zhilin, S.G. 2006. Early Miocene climate of Central Eurasia–Evidence from Aquitanian floras of Kazakhstan. *Palaeogeography, Palaeoclimatology, Palaeoecology* **248**, 32–48.

Bruch, A., Uhl, D. & Mosbrugger, V. 2007. Miocene climate in Europe–Patterns and Evolution. *In: A First Synthesis of NECLIME*. Palaeogeography, Palaeoclimatology, Palaeoecology **253**, 1–7.

Bruch, A., Utescher, T., Mosbrugger, V. & NECLIME members 2011. Precipitation patterns in the Miocene of Central Europe and the development of continentality. *In:* Utescher, T., Boehme, M. & Mosbrugger, V. (eds), *The Neogene of Eurasia: Spatial Gradients and Temporal Trends — The Second Synthesis of NECLIME*. Palaeogeography, Palaeoclimatology, Palaeoecology **304**, 202–211. doi:10.1016/j.palaeo.2010.10.002.

Chahlov, V.A. 1948. Materialy k poznaniju tretichnoy flory Zapadnoy Sibiri. *Annual Proceedings of Tomsk State University,* 1– 99.

Dorofeev, P.I. 1963. *Tretichnye Flory Zapadnoy Sibiri*. Moskva-Leningrad, **346**.

Eronen, J.T., Puolamäki, K., Liu, L., Lintulaakso, K., Damuth, J., Janis, C. & Fortelius, M. 2010. Precipitation and large herbivorous mammals II: application to fossil data. *Evolutionary Ecology Research* **12**, 235–248.

Fan, M., Songa, C., Dettman, D.L., Fang, X. & Xu, X. 2006. Intensification of the Asian winter monsoon after 7.4 Ma: Grain-size evidence from the Linxia Basin, northeastern Tibetan Plateau, 13.1 Ma to 4.3 Ma. *Earth and Planetary Science Letters* **248**, 186–197.

Fortelius, M., Eronen, J.T., Jernvall, J., Liu, L., Pushkina, D., Rinne, J., Tesakov, A., Vislobokova, I., Zhang, Z. & Zhou, L. 2002. Fossil mammals resolve regional patterns of Eurasian climate change during 20 million years. *Evolutionary Ecology Research* **4**, 1005–1016.

Gnibidenko, Z.N., Martynov, V.A., Donchenko, V.V. & Nikitin, V.P. 1989. Magnitostratigraphicheskiy razrez neogenovych otlozheniy Barabinskou ravniny. *Geology and Geophysics* **2**, 11–20.

Gnibidenko, Z.N. 2007. Paleomagnetism of the Late Cenozoic of the West Siberian Plate. *Geology and Geophysics* **48**, 431–445.

Gong, D.Y., Wang, S.W. & Zhu, J.H. 2001. East Asian winter monsoon and Arctic Oscillation. *Geophysical Research Letters* **28**, 2073–2076.

Gorbunov, M.G. 1955. Tretichnaja flora. *In: Atlas rukovodjashih form iskopaemyh fauny i flory Zapadnoy Sibiri*. Volume **2**. Moskva.

Gradstein, F.M., Ogg, J.G. & Smith, A.G. 2004. *A Geologic Time Scale 2004*. Cambridge University Press.

Guo, Z.T., Peng, S.Z., Hao, Q.Z., Biscaye, P., An, Z.S. & Liu, T.S. 2004. Late Miocene–Pliocene development of Asian aridification as recorded in the Red-Earth Formation in northern China. *Global and Planetary Change* **41**, 135–145.

Huang, Y., Clemens, S.C., Liu, W., Wang, Y. & Prell, W.L. 2007. Large-scale hydrological change drove the late Miocene C4 plant expansion in the Himalayan foreland and Arabian Peninsula. *Geology* **35**, 531–534.

International Stratigraphic Chart 2006. *International Commission on Stratigraphy*.

Knies, J. & Gaina, C. 2008. Middle Miocene ice sheet expansion in the Arctic: Views from the Barents Sea. *Geochemistry, Geophysics, Geosystems* **9**, Q02015.

Kovar-Eder, J. & Sun, G. 2009. The Neogene flora from Badaogou of Changbai, NE China – Most similar living relatives of selected taxa and relations to the European record. *Review of Palaeobotany and Palynology* **158**, 1–13.

Kryshtofovich, A.N. 1928. Novye dannye k verchnetretichnoy flore severozapadnoy sibiri. *Proceedings of the Geological Kommittee* **46**, p. 7.

Kuz'mina O.B. & Volkova B.S. 2008. Palynostratigraphy of Oligocene–Miocene continental deposits in Southwestern Siberia. *Stratigraphy and Geological Correlation* **16**, 540–552.

Laukhin, S., Grinenko, O. & Fradkina, A. 1992. Cenozoic climatic history of the arctic coast of Northeast Asia. *International Geology Review* **34**, 197–206.

Liu, Y.C., Utescher, T., Zhou, Z. & Sun, B. 2011. The evolution of Miocene climates in North China: preliminary results of quantitative reconstruction from plant fossil records. *In:* Utescher, T., Boehme, M. & Mosbrugger, V. (eds), *The Neogene of Eurasia: Spatial Gradients and Temporal Trends — the Second Synthesis of NECLIME*. Palaeogeography, Palaeoclimatology, Palaeoecology **304**, 308–317. doi:10.1016/j.palaeo.2010.07.004.

Lunt, J.D., Flecker, R., Valdes, J.P., Salzmann, U., Gladstone, R. & Haywood, M. A. 2008. A methodology for targeting palaeo proxy data acquisition: a case study for the terrestrial late Miocene. *Earth and Planetary Science Letters* **271**, 52–62.

Martynov, V.A., Gnibidenko, Z.N. & Nikitin, V.P. 2000. Besheulsky gorizont miotsena Zapadnoy Sibiri. *Stratigraphy and Geological Correlation* **8**, 78–87.

Micheels, A., Bruch, A.A., Uhl, D. & Mosbrugger, V. 2007. The global Tortonian vegetation and its influence on climate: Results from a sensitivity experiment with the AGCM ECHAM4/ML. *Palaeogeography, Palaeoclimatology, Palaeoecology* **253**, 251–270.

Micheels, A., Bruch, A.A. & Mosbrugger, V. 2009. Miocene climate modelling sensitivity experiments for different CO_2 concentrations. *Palaeontologia Electronica* **12**, Issue 2; 5A. 20 p.

Micheels, A., Bruch, A.A., Eronen, J., Fortelius, M., Harzhauser, M., Utescher. T. & Mosbrugger, V. 2011. Analysis of heat transport mechanisms from a Late Miocene model experiment with a fully coupled atmosphere–ocean general circulation model. *In:* Utescher, T., Boehme, M. & Mosbrugger, V. (eds), *The Neogene of Eurasia: Spatial Gradients and Temporal Trends — the Second Synthesis of NECLIME. Palaeogeography, Palaeoclimatology, Palaeoecology* **304**, 337350. doi:10.1016/j.palaeo.2010.09.021.

Mosbrugger, V. & Utescher, T. 1997. The coexistence approach–a method for quantitative reconstructions of Tertiary terrestrial palaeoclimate data using plant fossils. *Palaeogeography, Palaeoclimatology, Palaeoecology* **134**, 61–184.

Mosbrugger, V., Utescher, T. & Dilcher, L. D. 2005. Cenozoic continental climatic evolution of Central Europe. *In: Proceedings of the National Academy of Sciences* **102**, 14964–14969.

Müller, M.J. 1996. *Handbuch ausgewählter Klimastationen der Erde.* Trier University.

New, M., Lister, D., Hulme, M. & Makin, I. 2002. A high-resolution data set of surface climate over global land areas. *Climate Research* **21**, 1–25.

Nikitin, V. P. 1969. *Paleocarpologicheskiy metod*. Tomsk. **81.**

Nikitin, V.P. 1988. Floristitscheskie urovni Neogena Zapadnoy sibiri. *In: Geology and minerals of Western Siberia.* Novosibirsk, 155–156.

Nikitin, V.P. 1999. *Paleokarpologija i stratigraphija paleogena i neogena severnoy Asii. Thesis for a Doctor's degree*. Ministry of natural resources of Russia. Novosibirsk.

Nikitin, V.P. 2000. Revisia paleontologicheskich kollekziy po kvarteru juga Zapadnoy Sibiri. *In: Report of Palaeontological Stratigraphycal Group for Period 1999–2000*, Volume II, Novosibirsk, p. 470.

Nikitin, V.P. 2006. *Palaeocarpology and Stratigraphy of the Paleogene and the Neogene Strata in Asian Russia*. Novosibirsk.

Nikitin, V.P. 2007. Paleogene and Neogene strata in Northeastern Asia: paleocarpological background. *Russian Geology and Geophysics* **48**, 675–682.

Panagiotopoulos, F., Shahgedanova, M., Hannachi, A. & Stephenson, D.B. 2005. Observed trends and teleconnections of the Siberian high: a Recently declining center of action. *Journal of Climate* **18**, 1411–1422.

Qiang, X.K., Li, Z.X., Powell, C.M. & Zheng, H.B. 2001. Magnetostratigraphic record of the late Miocene onset of East Asian monsoon, and Pliocene uplift of northern Tibet. *Earth and Planetary Science Letters* **187**, 83–93.

Reinink-Smith, L.M. & Leopold, E.B. 2005. Warm climate in the late Miocene of the South Coast of Alaska and the occurrence of *Podocarpaceae* pollen. *Palynology* **29**, 205–262.

Rogers, J.C. 1997. North Atlantic storm track variability and its association to the North Atlantic Oscillation and climate variability of northern Europe. *Journal of Climate* **10**, 1635–1647.

Sloan, L.C. & Pollard, D. 1998. Polar stratospheric clouds: a high-latitude warming mechanism in an ancient greenhouse world. *Geophysical Research Letters* **25**, 3517–3520.

Stachura-Suchoples, K. & Jahn, R. 2009. Middle Miocene record of *Pliocaenicus changbaiense* sp nov. from Changbai (Jilin Province, China). *Acta Botanica Croatica* **68**, 211–220.

Steppuhn, A., Micheels, A., Bruch, A.A., Uhl, D. & Mosbrugger, V. 2007. The sensitivity of ECHAM4/ML to a double CO_2 scenario for the Late Miocene and the comparison to terrestrial proxy data. *Global and Planetary Change* **57**, 189–212.

Syabryaj, S., Utescher, T., Molchanov, S. & Bruch, A. 2007. Vegetation and palaeoclimate in the Miocene of Ukraine. *Palaeogeography, Palaeoclimatology, Palaeoecology* **253**, 169–184.

Takaya, K. & Nakamura, H., 2005. Mechanisms of intraseasonal amplification of the cold Siberian High. *Journal of Atmospheric Sciences* **62**, 4423–4440.

Thiede, J., Nørgaard-Pedersen, N. & Spielhagen, R. 1998. High-resolution stratigraphy of Upper Cenozoic northern high latitude glacial marine sediments. *Geoscience* **98**, 14–18.

Utescher, T., Bruch, A., Micheels, A., Mosbrugger, V. & Popova, S. 2011. Cenozoic climate gradients in Eurasia–a palaeo-perspective on future climate change? *In:* Utescher, T., Boehme, M. & Mosbrugger, V. (eds), *The Neogene of Eurasia: Spatial Gradients and Temporal Trends — the Second Synthesis of NECLIME*. Palaeogeography, Palaeoclimatology, Palaeoecology **304**, 351–358. doi: 10.1016/j.palaeo.2010.09.031.

Utescher, T., Djordjevic-Milutinovic, D., Bruch, A. & Mosbrugger, V. 2007. Palaeoclimate and vegetation change in Serbia during the last 30 Ma. *Palaeogeography, Palaeoclimatology, Palaeoecology* **253**, 157–168.

Utescher, T. & Mosbrugger, V. 2010. The Palaeoflora Database. http://www.palaeoflora.de.

Utescher, T., Mosbrugger, V. & Ashraf, A.R. 2000. Terrestrial climate evolution in Northwest Germany over the last 25 million years. *Palaios* **15**, 430–449.

Utescher, T., Mosbrugger, V., Ivanov D. & Dilcher, D. 2009. Present day climatic equivalents of European Cenozoic climates. *Earth and Planetary Science Letters* **284**, 544–552.

Vyssotski, A.V., Vyssotski, V.N. & Nezhdanovc, A.A. 2006. Evolution of the West Siberian Basin. *Marine and Petroleum Geology* **23**, 93–126.

Yakubovskaya, T.A. 1957. Novye nachodki tretichnoy flory v tomskom priob'e. *In: Proceedings of the Academy of Sciences of USSR* **116**, p. 2.

Yao, Y.F., Bruch, A.A., Mosbrugger, V. & Li, C.S. 2011. Quantitative reconstruction of Miocene climate patterns and evolution in Southern China based on plant fossils. *In:* Utescher, T., Boehme, M. & Mosbrugger, V. (eds), *The Neogene of Eurasia: Spatial Gradients and Temporal Trends — the Second Synthesis of NECLIME*. Palaeogeography, Palaeoclimatology, Palaeoecology **304***,* 291–307. doi:10.1016/j.palaeo.2010.04.012

Zachos, J.C., Pegani, U., Stone, L., Thomas, E. & Billups, K. 2001. Trends, rhythms, and aberrations in global climates 65 Ma to present. *Science* **292**, 686–693.

Zhang, Z., Wang, H. & Guo, Z. 2007. What triggers the transition of palaeoenvironmental patterns in China, the Tibetan Plateau uplift or the Paratethys Sea retreat? *Palaeogeography, Palaeoclimatology, Palaeoecology* **245**, 317–331.

Appendix

N collect.	Floras	Geographical Coordinates (longitude; latitude)	MAT min	MAT max	CMT min	CMT max	WMT min	WMT max	MAP min	MAP max	MPwetmin	MPwetmax	MPdry. min	MPdry. max	MPwarm min	MPwarm max
	Late Pliocene															
H2469	Mirny / Rannebarnaulsky[2]	82; 55	9.9	12.5	−0.3	0.7	18.8	24.6	676	1076	88	113	24	43	82	84
H4080	Merkutlinskiy / Rannebarnaulsky[2]	72; 56	7.3	16.2	−3.8	6.2	17.3	23.8	565	1213	84	167	16	38	66	95
H2245	Maly-shik / Rannebarnaulsky[2]	81; 54	4.4	7.3	−6.4	0.7	17.2	24.4	561	705	82	117	24	27	82	125
H2216	Logovskoy / Rannebarnaulsky[2]	81; 54	4.4	12.6	−11.5	3.5	17.2	24.4	631	971	91	113	16	32	66	68
H2460	Kabinet / Rannebarnaulsky[2]	80; 55	6.6	7.3	−4.4	4.6	21.6	24.4	631	705	103	168	24	27	82	95
H2646	Delyankir / Rannebarnaulsky[2]	133; 63	6.9	7.8	−6.9	1.3	18.9	24.9	594	971	103	139	24	32	82	84
H3398	Chernoluch'e / Andreevsky[1]	73; 55	5.4	7.3	−5.9	0.7	19.6	20.3	544	705	71	109	24	27	55	68
H3642	Blizkiy	162; 64	−0.6	11.1	−12.8	5.2	15.6	23.3	453	980	68	118	8	53	55	118
H3503	42km/ Rannebarnaulsky[1]	80; 55	6.6	11.1	−4.4	0.7	21.6	23.3	631	980	91	113	24	41	73	94
	Early Pliocene															
H3685	Tnekveem	177; 66	3.4	10.8	−11.8	5.8	18.9	25.6	592	1206	103	143	22	43	82	141
H2647	Hydzhak	147; 63	6.9	7.8	−8.7	1.3	18.8	24.9	453	1206	64	143	12	43	33	107
	Late Miocene															
H3690	Yanran	161; 68	1.8	16.1	−12.9	7.8	17.5	25.6	581	1206	91	143	12	32	82	141
H4967	Yana	149; 59	3.3	16.1	−8.1	6.4	15.9	25.6	581	1206	91	143	12	53	55	95
H4954	Temmirdekh-khaj	132; 71	9.3	10.8	−2.8	1.1	21.6	23.8	735	975	88	131	24	32	82	84
H4954	Omoloy	133; 70	7.3	16.1	−3.8	6.4	21.7	25.6	592	1206	102	143	18	32	82	143
H3658	Nekkeveem / early Chattian[3]	165; 69	1.8	15.6	−12.9	7.8	17.5	25.6	373	1206	82	143	8	32	82	143
H2811	Magadan	150; 59	3.3	16.1	−9.5	6.4	17.8	25.6	581	1206	98	143	9	26	92	143
H3681	Osinovaja	175; 64	9.1	16.1	−2.7	7.8	19.3	25.6	609	975	79	143	15	59	47	84
	Middle Miocene															
H3207	Yur'ev / Kaskovsky[1]	83; 58	9.5	13	−2.7	2.8	21.9	24.6	776	1322	103	168	32	43	78	83
H2283	Urozhay / Kaskovsky[1]	79; 53	9.5	13	−0.1	2.8	21.9	24.9	897	900	150	195	42	48	120	141
H4534	Rogozino / Kaskovsky[1]	69; 56	9.5	13	−0.1	2.8	22.3	23.3	776	971	116	118	32	43	92	95
H3459	Residentsiya	143; 59	3.4	16.1	−12.9	6.4	18.9	25.6	592	1206	103	143	22	53	74	120
H4044	Pokrov-ishym / Besheulsky[2]	68; 51	13.3	15.7	−0.1	6.2	24.9	25.1	776	1122	150	167	32	69	120	122

H3202	Orlovka / Novomikhaylovsky[2]	80; 55	13.3	17.5	–0.1	7.7	25	27.9	897	1146	108	139	22	50	84	95
H2570	Mamontova Gora / Kaskovsky[1]	133; 63	12.5	13.7	–0.1	1.3	21.6	24.7	776	847	150	195	32	32	120	141
H3673	Konachan / Isakovsky[1]	171; 65	9.1	16.4	–2.5	6.4	19.3	25.9	609	1322	116	195	22	61	82	154
H3192	Ivanovka / Langian[3]	76; 55	12.5	13	–0.1	2.8	21.9	24.6	776	1122	150	168	32	41	120	141
H2746	Borovljan / Isakovsky[1]	68; 56	9.1	13	–2.7	2.8	19.3	24.6	609	1322	103	168	24	69	58	95
H1297	Achair / Kaskovsky[1]	73; 54	12.5	13	–0.1	2.8	22.8	24.6	776	1122	150	180	41	43	120	141
84uv	Tambov	40; 50	14	21.7	–0.1	13.16	26.5	28.1	594	1281	116	265	24	43	89	172
12ss	Tambov	40; 52	15.7	20.8	2.2	13.6	25.6	28.10	897	900	109	109	50	67	84	87
33uv	Tambov	42; 51	13.3	14.7	–0.1	6.8	20.2	24.6	897	1281	150	168	50	67	120	141
	Early Miocene															
H1022	Yarsk / Aquitanian - Burdigallian[3]	84; 56	6.9	20.8	–6.9	13.3	19.3	28.4	631	1613	103	195	22	43	78	107
H3020	Voronovo / Tagansky[1]	83; 56	12.5	12.6	–0.1	4.4	24.9	24.9	776	1076	102	139	32	43	82	94
H3016	Voronovo / Kireevsky[1]	83; 56	12.5	13.3	–0.1	3.5	24.9	25.1	776	1076	103	113	32	57	82	88
H3065	Vilenka / Kireevsky[1]		9.1	20.8	–2.7	13.3	19.3	28.1	609	1322	103	195	22	43	78	195
H2906	Vasyugan / Vasjuganojarsky[1]	76; 58	5.4	16.4	–6.5	7.1	18.9	25.1	592	1520	103	167	22	43	78	120
H1689	V. dem'yan / Aquitanian[3]	75; 57	9.5	13	–0.1	2.8	21.9	24.9	776	1281	103	174	41	43	82	107
H4950	Ulan-kyu	133; 70	13.3	15.7	–0.1	6.4	21.6	25.6	592	1206	103	143	22	43	78	107
H2891	Perekatny yar / late Aquitanian[3]	76; 58	9.3	13	–2.7	2.8	21.6	24.9	592	1437	103	195	22	43	78	154
H2905	Ognev yar / Ekaterininsky[1]	76; 58	13.8	21.3	1.8	13.3	20.7	27.9	632	1281	103	195	24	43	58	107
H2894	Novy vasjugan / Aquitanian[3]	76; 58	11.2	13	–0.1	2.8	21.9	24.6	776	1146	150	168	32	43	120	141
H2818	Nadtsy / Ljaminsky[1]	68; 58	11.2	13	1.8	2.8	21.9	24.6	776	1281	150	168	32	67	120	141
H2895	Medvedkovo / late Aquitanian[3]	76; 58	9.1	20.8	–2.7	13.3	18.9	28.4	592	1520	103	195	22	67	58	195
H4490	Lyamin / late Aquitanian[3]	70; 62	9.5	13	–2.7	2.8	21.9	24.6	776	1322	103	168	32	43	82	95
H1683	Kulun'yah / Aquitanian[3]	76; 58	9.3	20.8	–2.7	13.3	21.5	28.1	609	1322	103	195	22	69	58	154
H502	Kozhevni / Tagansky	83; 56	12.5	13.3	–0.1	3.5	24.9	26.2	776	1076	103	113	32	43	82	94
H501	Kozhevni / Tagansky[1]	83; 56	12.5	13	–0.1	2.8	24.9	24.9	776	1281	116	167	32	43	82	122
H476	Kozhevni / Kireevsky[1]	83; 56	12.5	13	–0.1	2.8	24.9	24.9	631	1122	116	167	22	43	82	120
H3440	Konev yar / late Aquitanian[3]	76; 58	11.2	12.5	–0.1	0.7	21.9	24.6	776	1076	150	195	32	43	120	141
H2289	Kolpashovo / Aquitanian[3]	82; 58	9.3	16.4	–2.7	6.4	21.9	25.9	776	900	103	109	32	43	78	87
H2651	Koynatkhun	179; 65	–6.2	16.1	–26.8	6.4	15.9	25.6	407	1206	64	143	12	83	27	143
H1039	Kluchi / Tagansky[1]	79; 52	10	11.6	–0.1	0.2	24.9	24.9	631	816	116	177	22	32	82	141
H3404	Kireevskoe / Kireevsky[1]	84; 56	12.5	13	–0.1	2.8	24.9	24.9	648	900	150	170	22	25	120	141
H2879	Katyl'ga / Vasjuganojarsky[1]	76; 59	9.5	13	–6.4	2.8	20.2	24.6	594	1400	103	168	24	43	78	95

H1792	Indigirka	142;67	9.5	16.1	−2.8	6.4	21.9	25.6	776	1194	108	143	32	83	108	141
H1697	Gorelaya / Aquitanian[3]	73; 57	−7.7	27.7	−24.4	27	10.5	32	76	3151	46	389	9	165	39	258
H1510	Dovol'noe / Kireevsky[1]	79; 54	12.5	15.7	−0.1	6.4	24.9	25.6	776	1122	108	170	41	64	108	141
H514	Cherny yar / Ambrosimovsky[2]	87; 57	9.5	13	−2.7	2.8	21.9	24.6	776	1322	103	168	32	43	82	95
H2031	Berezovaja rechka / Aquitanian[3]	84.2; 56	13.3	16.4	−0.1	7.1	23	25.1	776	1281	150	167	32	50	74	107
H2030	Berezovaja rechka / Burdigalian[3]	84; 56	9.3	21.3	−2.8	17.8	21.5	28.3	305	1534	65	195	2	85	27	177
H2008	Barchan / Aquitanian[3]	84; 56	12.5	21.3	−0.1	13.3	24.9	28.1	776	1322	103	180	32	69	74	107
H4766	Amelich / Aquitanian[3]	80; 59	13.8	15.7	1.8	7.7	21.9	26.2	776	1146	103	139	32	64	82	95
Late Oligocene																
H1939	Zakharov		13.3	16.4	−0.1	6.2	24.9	26.2	776	1281	103	174	41	83	82	107
H3521	Tomsk / Basandaysky[1]	84; 56	13.3	15.7	−0.1	7.1	24.9	26.2	776	1281	122	174	41	43	108	141
H639	Lagerny sad / Zhuravsky[2]	84; 56	12.5	13	−0.1	2.8	21.9	24.9	897	1146	150	180	42	43	120	141
H4051	Lagerny sad / Zhuravsky[2]	84; 56	12.1	13	0.9	2.8	22.3	24.6	979	1134	150	180	42	43	120	148
H2285	Ozeryan / Zhuravsky[2]	78; 53	9.5	16.8	−6.5	9.6	20.2	28.2	338	1194	92	220	9	25	66	214
H4759	Nevol'ka / Zhuravsky[2]	79; 58	12.5	15.7	−0.1	7.1	24.9	25.9	776	900	109	109	32	48	82	87
H2009	Nelyubino / Zhuravsky[2]	84; 56	9.5	16.4	−2.7	7.1	21.9	25.1	776	1520	103	167	32	43	82	107
H1977	Mura / Basandaysky[1]	82; 56	13.3	15.7	−0.1	2.8	24.9	24.9	776	1281	109	180	41	43	82	107
H4152	Kompasskiy bor / Novomikhaylovsky[2]	83; 60	12.5	16.4	−0.1	7.1	24.9	25.6	776	1122	103	170	32	43	78	120
H3058	Ishym nagorny / Koshkulsky[1]	84; 56	14	14.7	−0.1	6.4	21.9	24.6	776	1213	116	168	41	43	78	95
H1953	Khmelevka / Koshkulsky[1]	83; 56	14	14.7	1.8	6.4	21.9	24.6	776	1213	116	168	41	43	82	95
H1926	Ermak	76; 52	13.3	17	−0.1	6.2	21.9	28.1	776	1281	102	195	41	64	82	154
H1952	Elegechevo	84; 56	9.5	20.8	−2.7	13.3	21.9	28.1	776	1322	92	195	41	43	82	154
H1120	Dubovka / Koshkulsky[1]	86; 54	12.5	15.7	3.8	7.1	24.9	25.6	1146	1322	150	170	41	64	120	141
H2000	Barkhan / Koshkulsky[1]	84; 56	13.3	14.7	−0.1	6.8	21.9	24.6	776	1281	103	168	41	43	82	95
H1123	Asino / Koshkulsky[1]	86; 56	13.3	17.7	−0.1	2.8	24.9	24.9	776	1281	116	180	41	43	82	107
Early Oligocene																
H1461	Voronovo / Novomikhaylovsky[2]	83; 56	11.2	14.7	3.8	6.4	21.6	24.6	1146	1281	103	195	24	27	85	95
H3048	Trubachovo / Altymsky[1]	84; 56	13.3	21.3	−0.1	13.3	21.6	27.9	592	1281	103	195	22	41	58	68
H4771	Pudino / Altymsky[1]	79; 57	9.5	14.7	−2.4	4.4	21.9	24.6	776	1400	108	139	32	43	82	83
H3434	Pozdnjakovo / Novomikhaylovsky[2]	84;56	9.1	20.8	−2.7	13.3	18.9	28.1	594	1520	103	195	24	67	58	154
H4036	Pavlograd / Altymsky[1]	73; 54	9.5	13	−0.1	2.8	21.7	24.9	592	1146	116	139	22	43	82	95
H1687	Obuhovka / Novomikhaylovsky[2]	72; 56	5.4	17.5	−6.9	7.7	18.9	27.9	592	1146	103	139	22	64	58	95
H4601	Novokolpakovo / Novomikhaylovsky[2]	82; 52	14	16.4	−0.5	7.1	24.7	26.2	776	1213	116	174	32	39	76	120

H2642	Nizhnya tavda / Altymsky[2]	66; 57	9.1	14.7	–2.7	4.4	18.9	24.6	592	1355	103	168	24	43	78	83
H3196	Lebyazh'e / Novomikhaylovsky[2]	71; 55	10.6	14.7	–2.8	6.4	21.5	24.6	413	1400	108	168	24	43	108	154
H4148	Kompasskiy bor / Novomikhaylovsky[2]	83; 60	9.5	11.6	–0.1	0.2	21.9	24.6	776	864	116	177	32	32	108	141
H3424	Kolarovo / Novomikhaylovsky[2]	84; 56	9.1	21.3	–2.7	13.3	18.9	28.6	592	1520	103	195	22	43	78	107
H1436	Katyl'ga / Novomikhaylovsky[2]	76; 59	13.3	18.7	–0.1	12.3	19.6	26.1	592	1281	103	195	22	43	58	83
H1940	Ekaterininskoe	74; 56	13.3	14.7	0.9	6.2	21.9	24.6	979	1281	106	168	41	43	90	95
H1269	Chumakaevka / Basandaysky[1]	82; 57	13.3	16.5	–0.1	6.4	24.9	27.4	776	1281	116	180	41	43	82	107
H2029	Berezovaja rechka / Novomikhaylovsky[2]	84; 56	12.5	15.7	–0.1	6.4	24.9	26.2	776	1520	103	174	32	43	82	120
H4768	Amelich / Novomikhaylovsky[2]	80; 59	9.3	14.7	–1.6	6.8	21.5	24.6	843	1400	122	195	41	43	78	83
H4770	Amelich / Altymsky[2]	80; 59	13.3	14.7	–0.1	6.8	21.9	24.6	776	1146	108	139	32	43	108	172
H3426	Ambartsevo / Novomikhaylovsky[2]	83; 57	9.3	13	–2.7	2.8	21.6	24.6	592	1400	103	168	24	43	78	95
H1289	Achair	73; 54	12.1	14.7	–1.1	6.4	21.9	24.6	776	1322	150	195	32	41	120	141
H914	Antropovo / Novomikhaylovsky[2]	65; 57	11.1	13	–0.1	2.8	21.9	24.6	1146	1281	131	168	53	64	85	95